Journal of Cultural Heritage 63 (2023) 158–168

Contents lists available at ScienceDirect

Journal of Cultural Heritage

journal homepage: www.elsevier.com/locate/culher

Original article

Non-invasive identification of red and yellow oxide and sulfide pigments in wall-paintings with portable ER-FTIR spectroscopy

Francesca Volpi[a,b,*], Mauela Vagnini[c,*], Riccardo Vivani[d], Marco Malagodi[a,b], Giacomo Fiocco[a,b]

[a] University of Pavia, Department of Musicology and Cultural Heritage, corso Garibaldi 178, 26100 Cremona, Italy
[b] University of Pavia, Arvedi Laboratory of Non-Invasive Diagnostics, CISRiC, via Bell'Aspa 3, 26100 Cremona, Italy
[c] Laboratorio di Diagnostica per I Beni Culturali, Piazza Campello 2, 06049 Spoleto, Italy
[d] University of Perugia, Department of Pharmaceutical Sciences, via del Liceo 1, 06123 Perugia, Italy

ARTICLE INFO

Article history:
Received 20 December 2022
Accepted 26 July 2023
Available online 12 August 2023

Keywords:
4–6: external reflection FTIR
Pigments
Wall painting
Non-invasive analysis
Cultural heritage

ABSTRACT

Scientific interest in analytical tools that enable reliable, repeatable, and rapid measurements without sampling is growing in the field of cultural heritage. Therefore, improving the use of methods that permit an efficient characterization of a wide range of materials through non-invasive and portable instruments, such as spectroscopies, is currently in high demand. This work is focused on the non-invasive study and identification of selected red and yellow pigments containing oxides and sulfides, frequently used in ancient wall-paintings, by means of portable External Reflectance Fourier Transform Infrared spectroscopy (ER-FTIR) within an extended spectral range (7500 - 360 cm^{-1}) which includes a portion of far IR addressing diagnostic peaks and band assignment for the first time. In this work we have also examined the reflection signals of the pigments when applied on a surface representing a fresco wall-painting, to discuss possible changes of the profile as the optical and morphological properties of the surface change.

For this purpose, yellow and red oxides, ochres, Siennas, minium, orpiment, and vermillion were selected and used to produce laboratory mock-ups of fresco paints. The ER-FTIR signals obtained on raw pigments were firstly validated by portable non-invasive Raman spectroscopy and X-Ray Fluorescence, and bench-top X-Ray powder Diffraction. Then, the results were subsequently compared with the ER-FTIR signals collected on the mock-ups to discuss the changes in the reflection spectral profile when in presence of rough surfaces and matrix-effects. The combined study on reference materials and mock-ups allowed to identify and discuss ER-FTIR marker bands which were finally validated on real samples of three fragments of Roman frescos provided by the Archeological Museum "San Lorenzo" in Cremona. The proposed method demonstrates distinctive IR features from external reflection analysis on the selected pigments, scarcely studied by portable FTIR instruments, offering a decisive advancement for in situ analytical characterization of the pigments used in wall-paintings.

Introduction

The human need to mark their presence with an artistic or functional approach has led to a specific search for durable-colored materials that could serve as pigments. Over the centuries many types of pigments, natural or synthetic, have been selected, produced, and applied, increasing progressively the artists' palettes [1]. Among them, mineral pigments such as yellow and red iron oxides, have always played a central role since antiquity due to their natural availability, high coloring capacity and stability under weather conditions [2,3]. The iron-based earth pigments, like ochres, Siennas, and umbers, were widely used in all periods in easel paintings, panels, and wall paintings. Similarly, lead oxides, arsenic and mercury sulfides have been used since the Roman period for red and yellow color introducing minium, realgar, orpiment, and cinnabar (or vermillion) pigments to the palette [4]. Accurate identification of ancient pigments is crucial for understanding the resources and technologies available in ancient societies, as well as for assessing the originality of the manufacts or planning conservation interventions. Recently, the use of non-

* Corresponding authors.
E-mail addresses: francesca.volpi@unipv.it (F. Volpi), m.vagnini@diagnosticabeniculturali.it (M. Vagnini).

https://doi.org/10.1016/j.culher.2023.07.019

invasive and portable instruments has been strongly encouraged in the field of cultural heritage to enable in situ investigation of immovable artworks such as wall paintings, statues, and large artifacts. Therefore, improving the recognition of heritage materials using direct, reliable, and non-invasive measurements is in high demand.

In this scenario, non-invasive portable spectroscopic techniques are ideal candidates due to their ability to rapidly obtain elemental or molecular information on a wide range of heritage materials, especially pigments. X-Ray Fluorescence (XRF), Raman and Fourier-Transform Infrared (FTIR) spectroscopies [5–13] have proven to be the standard techniques, in their portable and contactless version, capable of achieving information from a large selection of ancient pigments. Concerning XRF, it enables the recognition of pigment classes containing characteristic elements with a detectable atomic weight, but it cannot distinguish different pigments within the same chemical class, nor can it clearly characterize pigment mixtures [14]. Raman spectroscopy has shown reasonable efficacy in identifying and differentiating pigments with similar compositions, particularly red and yellow inorganic pigments [15–17], but the eventual presence of organic compounds, such as an organic binder, can produce large fluorescence signals that overlap with those of analytes.

Highly informative analytical responses are frequently gained through FTIR spectroscopy both for organic and inorganic compounds, including binders, varnishes, and pigments [18–21]. Among FTIR instruments, portable external reflection spectroscopy (ER-FTIR) is certainly promising in heritage science as it meets the requirements of portability, non-invasiveness, and sensitivity under various working conditions. Despite the technological advancement and analytical potentiality of ER-FTIR, benchtop instruments operating in the Far-IR range (FIR) are still often preferred [22–25] for the study of specific classes of pigments such as those containing oxides and sulfides, since these pigments show characteristic IR lattice vibrations below 900 cm^{-1} which lie outside the spectral range of many portable instruments proposed so far in heritage studies [26]. In addition, one of the main concerns of ER-FTIR instruments regards the correct interpretation of reflection spectra acquired on inhomogeneous surfaces, such as those of fresco wall-paintings. Here, the carbonate particles act as a binder for the pigment powder, strongly influencing both the optical properties and the morphology of the surface, namely the absorption coefficient, refractive index, and the scattering coefficient of the surface, producing distortions, shifts, enhancement, or disappearance of the bands [27,28]. For these reasons, the acquisition of spectral databases is often preferred for a tentative interpretation of reflection signals and band attribution.

Research aim

The present research aims (i) to create a reference study on selected red and yellow pigments containing oxides or sulfides, using portable ER-FTIR for the first time emphasizing data from a portion of the FIR region (600 −360 cm^{-1}); (ii) to investigate the changes of the spectral features when these pigments are applied on inhomogeneous surfaces such as those of fresco paintings. To this purposes yellow and red oxides, ochres, siennas, minium, orpiment, and vermillion were selected and used to produce laboratory mock-ups of fresco paintings based on historical recipes. ER-FTIR results obtained on raw pigments were previously analyzed by portable non-invasive Raman spectroscopy, XRF, and bench-top X-ray powder diffraction (XRD) to assess their actual composition. Finally, they were compared and discussed with those acquired on the mock-ups, and with those obtained on original fragments of Roman frescos which were provided by the Archaeological Museum “San Lorenzo ” in Cremona. This research is intended to contribute to the field of heritage science by providing an informed interpretation of reflection spectra in the presence of chemically inhomogeneous and morphologically rough surfaces such as those of ancient frescos.

Materials and methods

Materials

Ten inorganic pigments (Table 1) were selected according to their extensive use over the centuries in art history for red and yellow decorations in wall-paintings [4]. They were purchased from Kremer Pigmente GmbH & Co. (Aichstetten, Germany). For ER-FTIR analysis each pigment was prepared in pellet using 300 mg of powder compressed at 3 tons for 2 min; whilst for checking the purity degree Raman, XRF, and XRD analyses were performed on powders. Laboratory mock-ups of fresco paints were prepared (**Fig. S1** in Supporting Information) based on historical recipes [29] and with the support of experienced restorers. A mixture of 1:2 lime putty and 0.0–0.7 mm Botticino marble powder (CTS s.r.l, Italy) was prepared to form a lime mortar substrate on which, while still wet, each water-dispersed pigment was brushed. In addition, three fragments of mural Roman frescos were included in the study: two red fragments CRPM-12 and CRPM-15 (Domus del Ninfeo, 1st century B.C., excavated in Cremona during 2005–2008), and one yellow fragment CRCL-2 (Domus Romana, 1st century A.D., discovered and excavated in Cremona in 2014) currently conserved in the Archaeological Museum “San Lorenzo” in Cremona, Italy.

Fourier-Transform infrared spectroscopy in external reflection mode (ER-FTIR)

A portable Alpha spectrometer (Bruker Optics, Etringen, Germany; Billerica, MA, USA) equipped with a SiC globar source, a permanently aligned RockSolid interferometer with gold mirrors, and a DLaTGS detector was used. Measurements were performed in external reflection mode with a 23°/23° optical layout, at the working distance of 15 mm and a diameter of 3 mm. A minimum of three points of analysis were carried out for each sample in the range 7500–360 cm^{-1} with a spectral resolution of 4 cm^{-1}. For each point 145 spectra (3 min scan time) were acquired, averaged, and transformed in log(1/R) (R = reflectance) by OPUS 7.2 software package. A gold flat mirror was used as the background. The ER-FTIR spectra acquired on the mock-ups and original wall paintings are representative of the analyzed samples and were minimally manipulated with baseline subtraction and smoothing using OPUS 7.2.

X-Ray fluorescence (XRF)

XRF was performed with a portable energy-dispersive spectrometer ELIO (XG Lab, Milan, Italy; Bruker Optics, Billerica, MA, USA). The excitation source works with a rhodium (Rh) anode and the beam is collimated to the sample surface with a spot diameter of about 1.3 mm. XRF measurements were performed at 40 kV tube voltage, 40 μA tube current for 120 s, and 2048 acquisition channels. Data were processed by ELIO 1.6.0.29 software. It is worth clarifying that due to the working conditions used in this study, i.e. air as medium, the detection of elements with $Z < 17$ such as magnesium, aluminum, silicon, phosphorus, and sulfur results underestimated or even undetected [31].

Portable sequentially shifted excitation (SSE) Raman spectrometer

The BRAVO spectrometer (Bruker Corporation, Billerica, MA, USA) was used with a newly patented SSE™ (Sequentially Shifted Excitation, patent number US8570507B1) technology called to

Table 1
List of the pigments considered in this work. Chemical information derived from the producer data sheet.

Pigment	No.	Chemical information	Historical use [4,30]
Red iron oxide	48,100	Fe_2O_3	Since prehistoric times
Red ochre	11,575	Various iron oxides	Since prehistoric times
Burnt Sienna	40,430	Italian burnt Sienna is prepared by calcining raw Sienna	Since ancient Egypt
Vermillion	42,000	Artificial mineral pigment based on mercuric sulfide HgS	From ancient Egypt to 19th century
Minium	42,500	Pb_3O_4	From ancient Rome to 20th century
Yellow iron oxide	48,000	FeO(OH)	Since prehistoric times
Yellow iron oxide	40,301	$FeO(OH) + Al_2O_3 + SiO_4 + CaCO_3$	Since prehistoric times
Yellow ochre	11,573	Various iron oxides	Since prehistoric times
Raw Sienna	40,400	$Fe_2O_3 \cdot nH_2O + Al_2O_3\ MnO_2 + SiO_2 \cdot H_2O$	Since prehistoric times
Orpiment	10,700	As_2S_3	From ancient Egypt to 19th century

mitigate fluorescence [32–34]. The laser is slightly wavelength-shifted during the acquisition and three raw Raman spectra were recorded at each point. A proper algorithm recognizes the peaks that shift at different laser wavelengths as valid Raman peaks, while the non-shifting peaks are recognized as fluorescence (or absorbance) peaks, removing them. BRAVO spectrometer uses two lasers (DuoLaser™) at 785 and 830 nm and a power less than 100 mW, during the acquisition. Spectra were acquired with an acquisition time between 500 ms and 2 s and an accumulation between 5 and 100 scans. For all the measurements OPUS 7.7 was used to select the appropriate acquisition parameters.

X-Ray powder diffraction (XRD)

Diffractograms of pigment powder were recorded with a D8 Advance diffractometer in Bragg-Brentano geometry, equipped with a Lynxeye XE-T fast detector (Bruker AXS, Karlsruhe, Germany), Cu-Ka radiation operating at 40 kV and 40 mA, with a step size 0.0170° 2θ, and step scan 1 s. Identification of crystalline phases was performed with a search and match procedure with the help of the Bruker AXS Diffrac.Eva program release 2020, interfaced with the COD database. Quantitative analyses of crystalline phases have been performed applying the Rietveld method with the help of the Bruker AXS Topas Version 6 software. Figs. S2-S6 show the plots of the last cycle of refinements.

Results and discussion

Raman spectroscopy, XRD, and XRF analysis on pure pigments

The purity of the selected pigments was checked by XRF, XRD, and Raman spectroscopy, and the chemical and mineralogical composition is summarized in Table 2. Reds No. 48100 and 42000, and yellows No. 48000 and 10700 consisted in pure compounds: hematite, mercury sulfide, goethite, and arsenic trisulfide, respectively, by XRD and Raman analysis [35–37] (Figs. S7 and S8). The other pigments additionally contained silicate minerals such as quartz and/or clay minerals (muscovite and kaolinite) [38], and occasionally calcite as expected for ochres and Siennas. In agreement with XRD and Raman results, XRF revealed iron (Fe) as the major element in the pigments containing hematite or goethite, but in yellow No. 40301 calcium (Ca) was more abundant. Manganese (Mn) was diagnostic for Siennas [4], while silicon (Si) and potassium (K) for muscovite. Minor or trace amounts of Ca, titanium (Ti), and Si, can be related to clay minerals or to ferric oxide [36]. In vermillion, minium, and orpiment, mercury (Hg), lead (Pb), and arsenic (As) were the major elements respectively, while minor or trace elements as Ti, Ca, and Fe were probably due to impurities of accessory minerals used for the manufacturing of pigments [39,40].

ER-FTIR analysis of red pigments and mock-ups

In accordance with XRD and Raman measurements, hematite (α-Fe_2O_3) was detected by ER-FTIR in red No. 48100, ochre No. 11575, and Sienna No. 40430, as the principal mineral responsible for conferring the red color [41]. The reflection spectrum of this mineral (Fig. 1a–c) showed the characteristic vibrations of Fe-O in the FIR range which appeared as intense and broad inverted bands (or Reststrahlen bands) with minima around 540 and 470 cm^{-1}. The wavenumbers of the inverted bands were found comparable with those of the absorption bands from transmission or total attenuated reflectance measurements reported in literature permitting their assignment in Table 3.

In addition to hematite, ochres and earths can also contain kaolinite ($Al_2Si_2O_5(OH)_4$), gypsum ($CaSO_42H_2O$), chalk ($CaCO_3$), and quartz (SiO_2) depending on the source of the earth and the degree of processing which the pigment has undergone [42]. In ochre No. 11575 (Fig. 1b) indeed, stretching and bending modes of kaolinite and quartz were detected in the Mid-IR (MIR) region as Reststrahlen bands, as confirmed by XRD and Raman analysis. In addition, three weak broad bands were ascribed to the combination of stretching and bending modes of silicates. The 1995 cm^{-1} band is tentatively assigned to the combination of 1165 and 800 cm^{-1} stretches in quartz. The 1875 cm^{-1} band may be the combination of SiO_2 vibrations at 1165 and 700 cm^{-1}, while the combination of 1080 and 700 cm^{-1} gives the band at 1785 cm^{-1}. For this pigment also the Near-IR (NIR) range was helpful in identifying kaolinite due to its typical combination bands at 4533 cm^{-1} and stretching modes of OH at high wavenumbers (3700–3600 cm^{-1}).

Burnt Sienna derived from the calcination of natural raw Sienna, which is yellow in color due to the presence of goethite (α-FeOOH) and contains carbonates and silicates. When raw Sienna is burnt goethite is thermally converted to hematite changing its color to darker red hue [15] while the carbonate fraction is eliminated. Therefore, in accordance with XRD and Raman analysis, the ER-FTIR spectrum of burnt Sienna No. 40430 (Fig. 1-c) showed signals of hematite, quartz, and kaolinite similar to those of red ochre making it difficult to differentiate the two spectra. Despite their similarity, however, distinctive features were observed around 2045 cm^{-1}, likely an additional combination of the stretching at 1008 cm^{-1} and 1040 cm^{-1} of kaolinite.

Vermillion (HgS) shows characteristic absorptions in the low-wavenumber region but since ER-FTIR enables the detection of a portion of the FIR we observed a signal at the limit of the detector, around 360 cm^{-1} (Fig. 1-d), that was related to the absorption band at 346 cm^{-1} reported in literature [23]. Finally, minium No. 42,500 (Pb_3O_4) showed diagnostic inverted peaks between 530 and 370 cm^{-1} in Fig.1-e in addition to traces of hydrocerussite around 3540, 1745 and 1395 cm^{-1}, which suggest the production of minium from the hydrated lead-carbonate.

Fig. 1 also reports the reflection spectra acquired on the mock-up surfaces. It was expected that the presence of the lime mor-

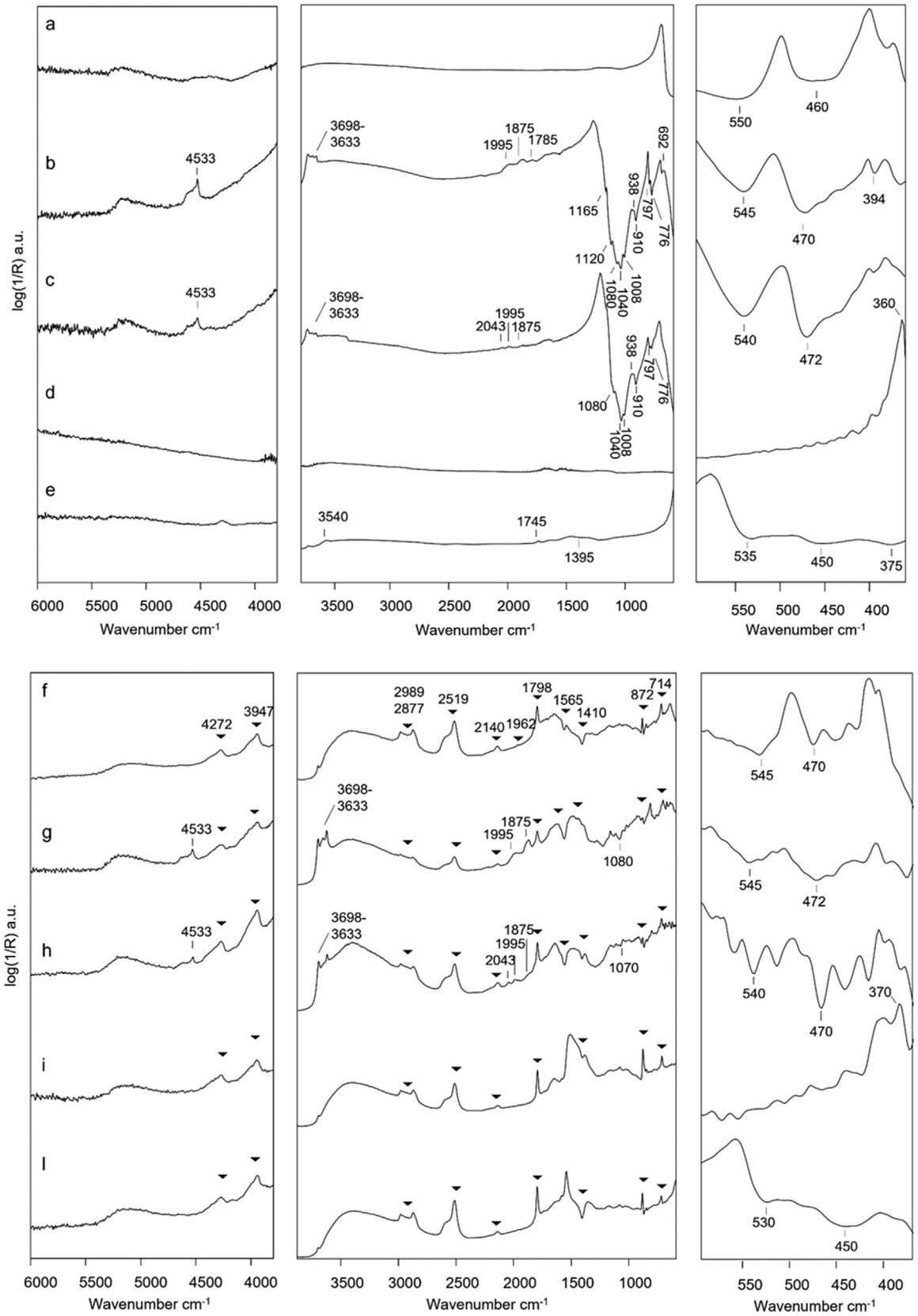

Fig. 1. ER-FTIR spectra of red pigments: (a) red iron oxide No. 48100, (b) red ochre No. 11575, (c) burnt Sienna No. 40430, (d) vermillion No. 42000, (e) minium No. 42,500. ER-FTIR spectra representative of fresco mock-up painted with the same pigments respectively in (f), (g), (h), (i), (l). The triangles correspond to the calcium carbonate peaks.

Table 2
XRF, XRD, and Raman analysis of the considered pigments. In XRF results, elements are reported in decreasing order of net area counts, and trace elements are in brackets. XRD measurements report the mineralogical phases (expressed by COD database) and their weight% obtained by Rietveld refinement procedures. Raman measurements report the identified compounds.

Pigment	Chemical and mineralogical composition			
	XRF	XRD	wt%	Raman
Red iron oxide No. 48100	Fe, Ti, Ca, Si, As (S, Mn)	Hematite COD 96–210–1168	100	Hematite
Red ochre No. 11575	Fe, Ti, Si, K (Ca, Zn, S, As)	Quartz COD 96–901–2601 Kaolinite COD 96–900–9231 Hematite COD 96–210–1168 Muscovite COD 96–901–2888	56 20 18 6	Quartz, hematite
Burnt Sienna No. 40430	Fe, Ti, Mn, Ca, Si (S, As, Pb)	Hematite Quartz Kaolinite Natrojarosite COD 96–901–0445 Gypsum COD 96–901–3167 Anatase COD 96–720–6076	40 20 16 12 8 4	Gypsum, hematite
Vermillion No. 42000	Hg, As, Ti, Ca, S (Fe, Si)	HgS COD 96–901–2083	100	Vermillion
Minium No. 42500	Pb, Ti, Ca (Fe, As)	Minium COD 96–901–2125	100	Minium
Yellow iron oxide No. 48000	Fe, Ti, Ca (S)	Goethite COD 96–900–2159	100	Goethite
Yellow iron oxide No. 40301	Ca, Fe, Ti, As, Si (S, Mn)	Calcite COD 96–900–9668 Goethite Gypsum Natrojarosite	83 14 2 1	Calcium carbonate, goethite
Yellow ochre No. 11573	Fe, Ti, Ca, Si (K, Zn, As)	Quartz Goethite Muscovite Kaolinite	47 34 12 7	Goethite, quartz
Raw Sienna No. 40400	Fe, Ca, Ti, Mn, As, Si (S, K)	Kaolinite Goethite Calcite Montmorillonite COD 96–900–2780 Quartz Anatase	37 22 20 15 3 3	Calcium carbonate, hematite, goethite
Orpiment No. 10700	As, S, Ti, Ca	As2S3 COD 96–900–8212		Orpiment

tar as a binder of the fresco paints introduced additional IR signals which could overlap, mask, or deform some bands of the pigment, while the roughness of the mock-up surface compared to the flat and smooth pellet, would favor the volume reflection over the surface one as studied by other authors [28,47]. Due to the interference of the lime mortar in the matrix of the mock-up additional bands of CO_3^{2-} vibrations appeared at 4272 cm^{-1} (3 ν_3 [44), 3946 cm^{-1} ($\nu_1 + 2\ \nu_3$) [48], 2989 and 2877 cm^{-1} (2 ν_1), 2519 cm^{-1} ($\nu_1 + \nu_3$), 2144 cm^{-1} ($\nu_4 + \nu_3$), 1962 cm^{-1} (ν_{3+} ν_2), 1798 cm^{-1} ($\nu_1 + \nu_4$) [49], 1565 and 1410 cm^{-1} (Reststrahlen band ν_3 [47]), 872 and 712 cm^{-1} (ν_2 and ν_4, respectively [44]). However, position and shape of the inverted bands of hematite at around 540 and 470 cm^{-1} remained unchanged in the analysis of mock-ups since no overlapping or odd interference with lime mortar occurred in the FIR range. Conversely, the MIR region was the most affected. The intense Reststrahlen bands of silicates between 1160 and 700 cm^{-1} were not clearly detected on the surface painted with red ochre No. 11575 and burnt Sienna No. 40430 (Fig. 1g, h) because the roughness of the surface generates a non-optically flat surface that promotes volume reflection over the specular one and the Reststrahlen bands appeared poorly intense [47]. The presence of silicates was therefore confirmed by the combination and overtone bands at 2050 (in burnt Sienna), 1995, and 1875 cm^{-1}, which due to the small absorption indexes they were enhanced by volume reflection providing, especially in this case, useful markers for the identification of the respective pigments. Identification of kaolinite was achieved only by its characteristic NIR signals at 4533 cm^{-1} and those at 3700–3600 cm^{-1} where no interference with the lime mortar was observed.

The areas painted with vermillion and minium (Fig. 1i and l, respectively) displayed reflection signals at the same frequencies observed for the pellets, in addition to those of the lime mortar. It is worth noting that the analysis of sulfide pigments, such as vermilion, does not provide signals in the most exploited MIR range, while allowing the use of a portion of the FIR may provide the detection of weak but diagnostic signals.

ER-FTIR analysis on yellow pigments and mock-ups

ER-FTIR spectra acquired on yellow pigments are shown in Fig. 2a-e with the corresponding bands attribution summarized in Table 4. The mineral goethite (α-FeOOH) was the principal chromophore of the areas painted with yellow iron oxide No. 48000, ochre No. 11573, and raw Sienna No. 40400 (Fig. 2f, h, i), characterized by the inverted bands around 900, 800, 680, 465, 420 and 400 cm^{-1}. As previously observed for the red pigments, the Reststrahlen bands are centered at the maximum of the absorbance bands reported in literature, addressing the bands assignment in Table 4.

Consistently with Raman and XRD results other minerals were recognized in addition to goethite in yellow No. 40,301, ochre No. 11,573, and Sienna No. 40,400. Moreover, it was observed that the

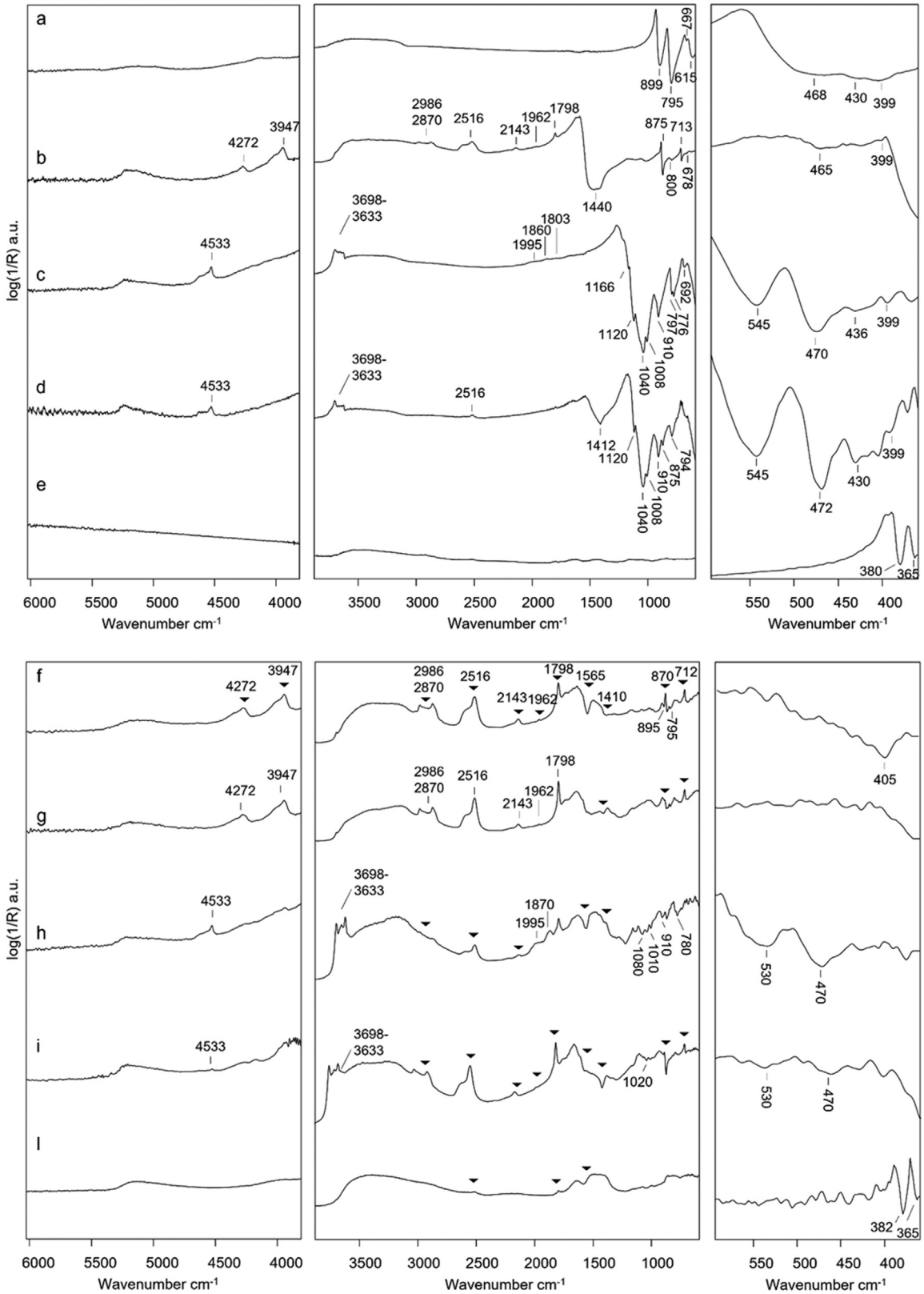

Fig. 2. ER-FTIR spectra of yellow pigments: (a) yellow iron oxide No. 48000, (b) yellow iron oxide No. 40301, (c) yellow ochre No. 11573, (d) raw Sienna No. 40400, (e) orpiment No. 10700. ER-FTIR spectra representative of fresco mock-ups painted with the same pigments, respectively in: (f), (g), (h), (i), (l). The triangles correspond to the calcium carbonate marker peaks.

Table 3
ER-FTIR bands assignment for red pigment pellets.

Pigment pellet	Band (cm^{-1})	Band assignment	Reference
Red iron oxide No. 48100	600–530	ν(Fe-O)	[25,42,43]
	460 inverted bands	δ(Fe-O) in hematite	
Red ochre No. 11575	4533	$\nu + \delta$(OH)	[44]
	3698–3633	νOH in kaolinite	
	1995, 1875, 1785	combination bands in quartz	[45]
	1165, 1120	ν_{as}(Si-O-Si)	
	1080	ν_{as}(Si-O)	[15,17,36]
	797, 776	ν_s(Si-O)	
	692 inverted bands	δ(Si-O) in quartz	
	1040	ν(Si-O-Si)	
	1008	ν(Si-O-Al)	
	938, 910 inverted bands	δ(Al-OH) in kaolinite	
	545	ν(Fe-O)	[25,43]
	470 inverted bands	δ(Fe-O) in hematite	
	394, 365 inverted bands	SiO_4- SiO_4 coupling in silicate	[36]
Burnt Sienna No. 40430	4533	$\nu + \delta$(OH)	[44]
	3698–3633	νOH in kaolinite	
	2043	combination band in kaolinite (tentative assignment)	[45]
	1995, 1875	combination bands in quartz	
	1166	ν_{as}(Si-O-Si)	[15,17,36]
	797, 776 inverted bands	ν_s(Si-O) in quartz	
	1040	ν(Si-O-Si)	
	1008	ν(Si-O-Al)	
	938, 910 inverted bands	δ(Al-OH) in kaolinite	
	540	ν(Fe-O)	[25,43]
	472 inverted bands	δ(Fe-O) in hematite	
Vermillion No. 42000	360 (peak max)	ν(Hg-S)	[23]
Minium No. 42500	3540, 1745 (weak), 1395 (very weak inverted band)	ν(OH), $\nu_1 + \nu_4(CO_3^{2-})$, ν_3 (CO_3^{2-}) in hydrocerussite	[44]
	530, 450, 375 inverted bands	ν(Pb-O)	[46]

presence of calcite or silicates in the pigment composition partially masked the signals of goethite around 900 and 700 cm^{-1}, allowing detection of the yellow mineral mainly through the FIR range. The ER-FTIR spectrum of orpiment No. 10,700 (Fig. 2e) showed two distinguishable peaks with minima at 380 and 365 cm^{-1} ascribable to the As-S stretching since Raman and XRD measurements confirmed the presence of solely orpiment. As was pointed out for vermilion, the vibration of sulfides occurs at low wavenumbers making it impossible to detect their signals with common portable FTIR instruments limited to 900 cm^{-1}, however, in this case the orpiment provided specific peaks that allow identification of this pigment.

In the reflection spectra acquired on the yellow mock-up paints in Fig. 2f-l we observed similar behaviors to those previously described for the reds. The Reststrahlen bands of goethite were mostly visible in the FIR range due to the partial overlap with those of silicates and calcite between 900 and 700 cm^{-1} described above. They appeared with the minimum at the same wavenumber of the reference pellet, implying that no shift or deformation occurred in presence of the matrix lime mortar. Quartz and kaolinite were identified in ochre No. 11573 and Sienna No. 40400 by their combination bands in the MIR and NIR more than by the Reststrahlen bands. As previously observed in the red mockups, the roughness of the surface favored the predominance of volume reflection that enhances the combination bands, rather than the specular reflection observed in the pellet surface, offering the possibility of using these bands as diagnostic features in real wall paint surfaces.

Finally, Fig. 2f revealed the diagnostic peaks of orpiment at the same wavenumbers as those of the pellet. For the sake of clarity, it is important to point out that the detection of sulfide pigments with portable FTIR is challenging and with our ER-FTIR instrument we were able to obtain weak but distinguishable signals from instrumental noise at the very limit of the working range of the detector. This condition, however, may create limitations and fail in the analysis of multicomponent surfaces or pigment mixtures not considered in this work.

Non-invasive analysis of Roman frescos by ER-FTIR

To validate the results obtained with the experimental method, the identification of red and yellow pigments using a portable ER-FTIR was carried out on three original fragments of Roman frescos (Fig. 3). The fragments were part of the sumptuous and fine wall decorations of two *domus* built between the end of the 1st century B.C. and the beginning of the 1st A.D. in the center of Cremona (Northern Italy), that by the end of the 1st century B.C. become a *municipium* of Rome. The walls of the *domus* were decorated with geometric, floral, and mythological motifs that suggested the expertise of a painter of high competence probably requested from Rome for his skill in the great decorative sites of the Augustan age. Indeed, the quality and the subject of the decorations reflected the remarkable economic and cultural level that the city of Cremona had reached, and the close connection with the politics of Rome [53].

Fragments CRPM-12, CRPM-15, and CRCL-2 were analyzed with ER-FTIR without any preparation and the results are reported here. The spectrum of the red fragment CRPM-12 (Fig. 3a) showed in the NIR and MIR ranges the peaks of calcium carbonate at 4272, 2986, 2870, 2516, 2143, 1795 cm^{-1} (overtones and combination bands), 1410, 874 and 712 cm^{-1} (Reststrahlen and derivative-like bands). Additional signals around 855 and 730 cm^{-1} suggested the presence of other carbonate than calcium carbonate, possibly dolomite [54], a calcium and magnesium carbonate also revealed in other Roman wall paintings [40]. The inverted bands between 1070 and 1010 cm^{-1} belong to silicates, likely quartz, while the presence of kaolin is uncertain due to the lack of the diagnostic signals at 4533 cm^{-1}. At lower wavelength the bands around 530 and 470 cm^{-1} of hematite were clearly identified. It was therefore hypothesized the use of iron-based pigments, probably a red

Table 4
ER-FTIR bands assignment for yellow pigment pellets.

Pigment	Band (cm^{-1})	Band assignment	Reference
Yellow iron oxide No. 48000	899, 795 inverted bands	δ(OH) in goethite	[36,50]
	667 (weak), 615	ν(Fe-O)	[15,24,43,50]
	468 (shoulder)	ν(Fe-O) or ν(Fe-OH)	
	399 inverted bands	ν(Fe-OH) in goethite	
Yellow iron oxide No. 40301	4272	$3\nu_3$ in calcite	[51]
	3947	$\nu_1 + 2\ \nu_3$ in calcite	[48]
	2986, 2870	$2\ \nu_3$	[44]
	2516	$\nu_1 + \nu_3$	
	2143	$\nu_4 + \nu_3$	
	1962	$\nu_2 + \nu_3$	
	1798	$\nu_1 + \nu_4$ in calcite	
	1470–1430 inverted band	ν_3 in calcite	
	872	ν_2	
	712 derivative-like bands	ν_4 in calcite	
	800	δ(OH)	[15,24,43,50]
	678, 465	ν(Fe-O)	
	400 inverted bands	ν(Fe-OH) in goethite	
Yellow ochre No. 11573	4533	$\nu + \delta$(OH)	[44]
	3698–3633	ν(OH) in kaolinite	
	1995, 1860	Combination bands of quartz	[45]
	1166, 1120	ν_{as}(Si-O-Si)	[15,17,36]
	1080	ν_{as}(Si-O)	
	797, 776	ν_s(Si-O)	
	692 inverted bands	δ(Si-O) in quartz	
	1040	ν(Si-O-Si)	
	1008	ν(Si-O-Al)	
	910 inverted bands	δ(Al-O-H) in kaolinite	
	545	ν(Fe-O)	[15,24,43,50]
	470	δ(Fe-O)	
	400 inverted bands	ν(Fe-OH) in goethite	
Raw Sienna No. 40400	4533	$\nu + \delta$(OH)	[44]
	3698–3633	ν(OH) in kaolinite	
	2516	$\nu_1 + \nu_3$	
	2143	$\nu_4 + \nu_3$	
	1798 (weak)	$\nu_1 + \nu_4$ in calcite	
	1412 inverted band	ν_3	
	874, 711 derivative-like	ν_2, ν_4 in calcite	
	1120 inverted band	ν_{as}(Si-O-Si) in quartz	[15,17,36]
	1040	ν(Si-O-Si)	
	1008	ν(Si-O-Al)	
	910 inverted bands	δ(Al-O-H) in kaolinite	
	794 inverted band	ν(Si-O) in quartz and/or goethite	
	545, 472	ν(Fe-O), δ(Fe-O)	[15,24,43,50]
	430, 400 inverted bands	ν(Fe-OH) in goethite	
Orpiment No. 10700	380, 365 inverted bands	ν(As-S)	[52]

earth pigment also containing silicates, as observed in the fresco mockup. The ER-FTIR results were supported by XRF analysis in Table S1 (Supporting Information). Calcium (Ca) and iron (Fe) were the major elements detected: Ca was attributed to the lime mortar of the fresco, Fe to hematite. Minor elements were strontium (Sr), which is generally vicarious of calcium present in the lime mortar, and silicon (Si) confirming the presence of silicates. Traces of manganese (Mn) were attributed to an earth pigment, in accordance with the hypothesis that the pigment used may have been a red ochre. The occurrence of mercury (Hg) and sulfur (S) in low abundance was due to the layer underneath colored with the addition of vermillion (data not reported).

Similarly, the red fragment CRPM-15 (Fig. 3b) displayed in the NIR and MIR the reflection signals of carbonates, although calcium carbonate seemed the predominant mineralogical species. Silicates were also identified by the typical Reststrahlen bands between 1700 and 1000 cm^{-1}. The FIR range allowed detecting two inverted bands at 530 and 472 cm^{-1} in addition to a signal with the maximum around 360 cm^{-1} suggesting the presence of both hematite and vermillion. This outcome was successfully confirmed by XRF measurements that revealed Hg as the predominant element, in conjunction with S, although the counts of S may result underestimated by our XRF working conditions because its secondary radiations can be severely attenuated by the air and/or any dense material superimposed [31,55]. In addition to Ca, Fe and Si were minor components possibly related to an iron-based pigment in a mixture with cinnabar, or underneath cinnabar, as reported by other authors [56]. It is worth highlighting that XRF confirmed vermillion as the principal red pigment in CRPM-15, along with a lower occurrence of an iron-based pigment, and that ER-FTIR successfully revealed and identified both in the FIR range. However, coupling ER-FTIR with XRF (or other spectroscopies) may still be required for confirming the presence of cinnabar.

Finally, in the yellow fragment CRCL-2 (Fig. 3c) calcium carbonate (4272, 2986, 2870, 2516, 2143, 1795, 1413, 875, 712 cm^{-1}) and quartz (1070 and 760 cm^{-1}) were mostly recognized in the high-wavelength regions, while the yellow chromophore below 900 cm^{-1}. Here, goethite clearly showed its typical spectral features around 900, 790, 475, 420–405 cm^{-1} confirming, in agreement with the previous observations on the fresco mock-up, the ability of ER-FTIR to detect and chemically discriminate among the class of iron-based pigments.

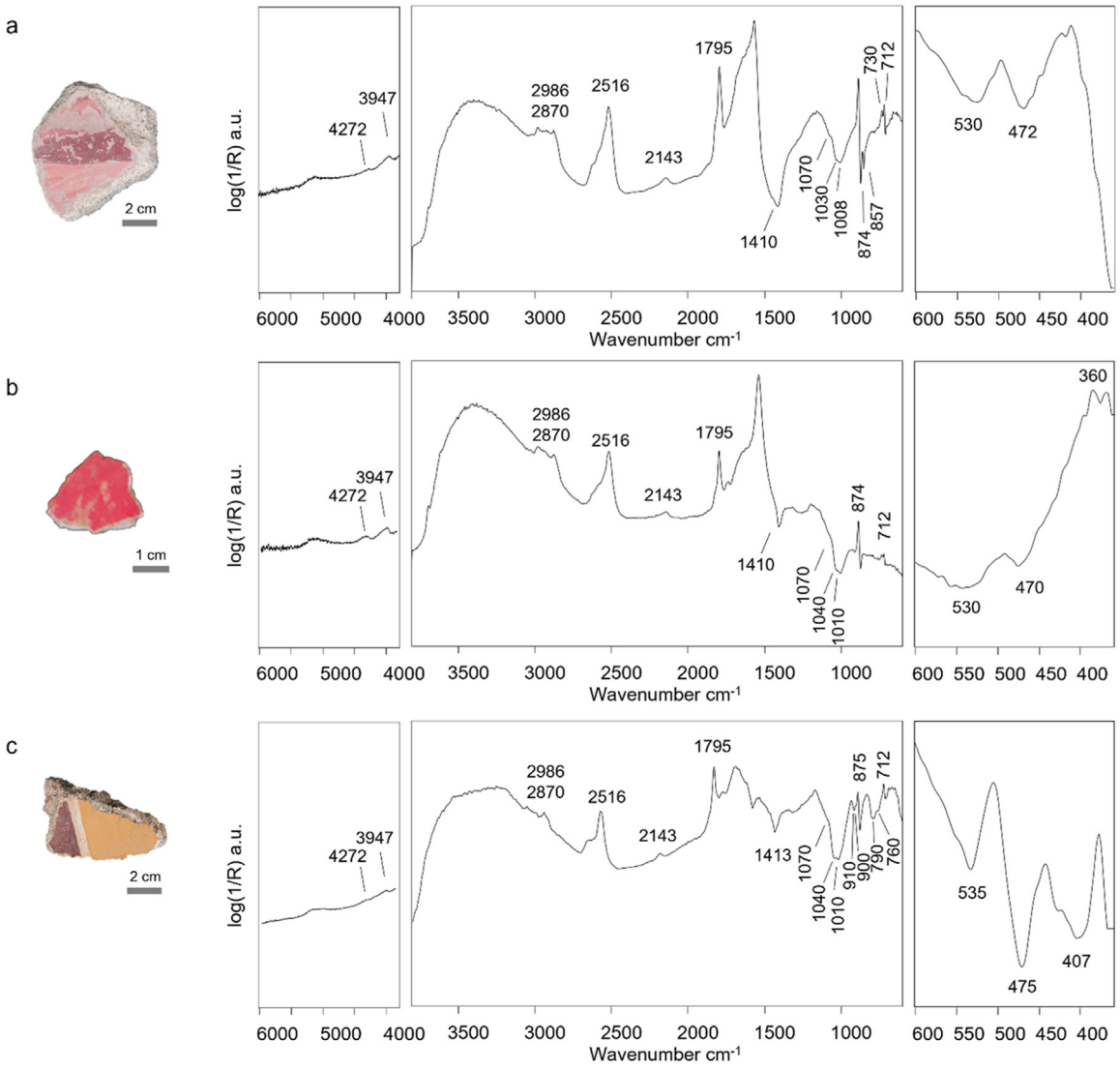

Fig. 3. Fragments of Roman frescos and relative ER-FTIR spectra of: (a) CRPM-12 (analyses were acquired on the dark red area), (b) CRPM-15, and (c) CRCL-2 (analyses were acquired on the yellow area).

The outcomes of the analytical investigation of the pigments of Cremona's *domus* were comparable to the mural paintings of the imperial court of Augustus in Rome. The use of iron-based pigments for reds or yellows was quite common in that period due to the ubiquity of these minerals and the affordable price, while the use of cinnabar for painting a large wall of the *domus* reflects the economic prosperity and the high social status of the patrons of the Cremonese *domus*.

Conclusions

This study explores the great potential of the non-invasive approach using portable ER-FTIR in the range 7500–360 cm^{-1}, besides Raman and X-ray spectroscopies, for the analysis of selected mineral pigments used in ancient wall-paintings. ER-FTIR has proved effective for the identification of oxide and sulfide pigments that absorb below 900 cm^{-1}, namely red and yellow iron oxides, ochres and earths, minium, vermillion, and orpiment, for which the reflectance features and band assignment was here presented for the first time. Indeed, only extending the detection range until a portion of the FIR the recognition of the chromophores such as hematite, goethite, and sulfides was allowed. The MIR region instead permitted the detection of silicates and carbonates by the characteristic Reststrahlen and combination bands, and the NIR mostly helped in the specific identification of kaolinite. Furthermore, this study detailed the modifications of the reflection spectral profile that occur when a pigment is applied with the fresco technique in comparison to the raw pigment, contributing to a mindful interpretation of reflection spectra acquired on rough and inhomogeneous surfaces, such as those of wall-paintings. Thanks to the experimental comparison between the raw pigments and the fresco mock-ups we were able to mainly observe: (a) no significant shift of the Reststrahlen bands; (b) overlapping or masking of some pigment bands with those of the lime mortar; (c) enhancement of the intensities of combination and overtone bands in the mock-ups. This latter case provided marker bands for the identification of specific silicate-containing pigments. Finally, non-contact ER-FTIR analysis was successfully applied to the non-invasive and direct characterization of reds and yellows in Roman fresco fragments demonstrating that the method was able to distinguish not only pigments containing oxides and sulfides but also within the iron-based class. The results proved promising for the identification of unknown pigments used in historical artifacts and different surface morphologies although the combined use of elemental

analysis may still be required for complex surfaces or mixture of pigments, especially when in presence of sulfide-based pigments.

Acknowledgements

We would like to thank Prof. Curzio Merlo (Laboratorio di Diagnostica e analisi chimico-fisiche of Scuola di Restauro CR. Forma, Cremona, Italy) for providing the tools to prepare the pigments pellet, Prof. Luciana Festa (Conservazione e Restauro dei Beni Culturali, University of Pavia, Cremona Campus, Italy) for the technical support in the preparation of the mock-ups. We are grateful to Elena Mariani (Archaeologist specialized in Roman Frescos at the Archaeological Museum "San Lorenzo" in Cremona), Marina Volonté (Museum conservator at the Archaeological Museum "San Lorenzo" in Cremona), and Dr. Nicoletta Cecchini (Soprintendenza Archeologia, Belle Arti e Paesaggio per le province di Cremona, Lodi e Mantova) for authorizing and supporting the study of the Roman fresco fragments.

Fundings

The research received no external funding from public, commercial, or non-profit sectors.

Author contributions

The work was originally designed by Volpi Francesca (V.F.), Vagnini Manuela (V.M.), and Malagodi Marco (M.M.); Material preparation, data collection, analysis, and interpretation were performed by V.F.; Raman analysis and interpretation were performed by V.M.; XRD measurements and results were carried out by Vivani Riccardo (V.R.); The first draft of the manuscript was written by V.F., subsequent versions of the manuscript were commented, reviewed, and edited by V.F., V.M., and Fiocco Giacomo (F.G.); The manuscript was validated by V.M., M.M., F.G.; All the authors reviewed and approved the final manuscript.

Supplementary materials

Supplementary material associated with this article can be found, in the online version, at doi:10.1016/j.culher.2023.07.019.

References

[1] J.R. Barnett, S. Miller, E. Pearce, Colour and art: a brief history of pigments, Opt. Laser Technol. 38 (2006) 445–453, doi:10.1016/j.optlastec.2005.06.005.
[2] B.H. Berrie, Artists' Pigments: A handbook of Their History and Characteristics, National Gallery of Art Washington, DC, USA, 2007 Vol 4.
[3] K. Helwig, The characterisation of iron earth pigments using infrared spectroscopy, in: B. Pretzel (Ed.), Second Infrared and Raman Users Group Conference (IRUG2) Victoria & Albert Museum (V&A), London, UK, 1998, pp. 83–92.
[4] N. Bevilacqua, L. Borgioli, I. Adrover Gracia, I pigmenti nell'arte dalla preistoria alla rivoluzione industriale. Il Prato ed.; 2010.
[5] F. Pozzi, A. Rizzo, E. Basso, et al., Portable spectroscopy for cultural heritage, in: R Crocombe, P Leary, B Kammrath (Eds.), Portable Spectroscopy and Spectrometry, Wiley, 2021, pp. 499–522, doi:10.1002/9781119636489.ch43.
[6] G. Fiocco, C. Invernizzi, S. Grassi, et al., Reflection FTIR spectroscopy for the study of historical bowed string instruments: invasive and non-invasive approaches, Spectrochim. Acta - Part A Mol. Biomol. Spectrosc. 245 (2021) 118926, doi:10.1016/j.saa.2020.118926.
[7] C. Invernizzi, G. Fiocco, M. Iwanicka, et al., Surface and interface treatments on wooden artefacts: potentialities and limits of a non-invasive multi-technique study, Coatings 11 (2021) 1–24, doi:10.3390/coatings11010029.
[8] L. Bonizzoni, S. Bruni, M. Gargano, et al., Use of integrated non-invasive analyses for pigment characterization and indirect dating of old restorations on one Egyptian coffin of the XXI dynasty, Microchem J. 138 (2018) 122–131, doi:10.1016/j.microc.2018.01.002.
[9] F. Casadio, C. Daher, L. Bellot-Gurlet, Raman Spectroscopy of cultural heritage materials: overview of applications and new frontiers in instrumentation, sampling modalities, and data processing, Top. Curr. Chem. 374 (2016), doi:10.1007/s41061-016-0061-z.
[10] A. Rousaki, P. Vandenabeele, In situ Raman spectroscopy for cultural heritage studies, J. Raman Spectrosc. 52 (2021) 2178–2189, doi:10.1002/jrs.6166.
[11] C. Germinario, F. Izzo, M. Mercurio, A. Langella, Multi-analytical and non-invasive characterization of the polychromy of wall paintings at the Domus of Octavius Quartio in Pompeii, Eur. Phys. J. Plus 133 (2018) 1–12, doi:10.1140/epjp/i2018-12224-6.
[12] C. Clementi, V. Ciocan, M. Vagnini, Non-invasive and micro-destructive investigation of the Domus Aurea wall painting decorations, Anal. Bioanal. Chem. 401 (2011) 1815–1826, doi:10.1007/s00216-011-5250-6.
[13] A.L.Q. Baddini, J.L.V.P. Santos, R.R. Tavares, L.S. Paula, H.D.C.A. Filho, R.P. Freitas, PLS-DA and data fusion of visible Reflectance, XRF and FTIR spectroscopy in the classification of mixed historical pigments, Spectrochim. Acta A Mol. Biomol. Spectrosc. 265 (2022) 1–9, doi:10.1016/j.saa.2021.120384.
[14] B. Beckhoff, B. Kanngießer, N. Langhoff, R. Wedell, H. Wolff, Handbook of Practical X-ray Fluorescence Analysis, Springer, 2006, doi:10.1007/978-3-540-36722-2.
[15] C. Montagner, D. Sanches, J. Pedroso, M.J. Melo, M. Vilarigues, Ochres and earths: matrix and chromophores characterization of 19th and 20th century artist materials, Spectrochim. Acta - Part A Mol. Biomol. Spectrosc. 103 (2013) 409–416, doi:10.1016/j.saa.2012.10.064.
[16] L. Burgio, J.R. Clark, Library of FT-Raman spectra of pigments, minerals, pigment media and varnishes, and supplement to existing library of Raman spectra of pigments with visible excitation, Spectrochim. Acta Part A Mol. Biomol. Spectrosc. 57 (2001) 1491–1521, doi:10.1016/S1386-1425(00)00495-9.
[17] D. Bikiaris, S. Daniilia, S. Sotiropoulou, et al., Ochre-differentiation through micro-Raman and micro-FTIR spectroscopies: application on wall paintings at Meteora and Mount Athos, Greece. Spectrochim. Acta - Part A Mol. Biomol. Spectrosc. 56 (2000) 3–18, doi:10.1016/S1386-1425(99)00134-1.
[18] F. Rosi, A. Daveri, C. Miliani, et al., Non-invasive identification of organic materials in wall paintings by fiber optic reflectance infrared spectroscopy: a statistical multivariate approach, Anal. Bioanal. Chem. 395 (2009) 2097–2106, doi:10.1007/s00216-009-3108-y.
[19] R. Ploeger, D. Scalarone, O. Chiantore, Non-invasive characterisation of binding media on painted glass magic lantern plates using mid-infrared fibre-optic reflectance spectroscopy, J. Cult. Herit. 11 (2010) 35–41, doi:10.1016/j.culher.2009.01.005.
[20] T. Poli, O. Chiantore, M. Nervo, A. Piccirillo, Mid-IR fiber-optic reflectance spectroscopy for identifying the finish on wooden furniture, Anal. Bioanal. Chem. 400 (2011) 1161–1171, doi:10.1007/s00216-011-4834-5.
[21] C. Invernizzi, A. Daveri, M. Vagnini, M. Malagodi, Non-invasive identification of organic materials in historical stringed musical instruments by reflection infrared spectroscopy: a methodological approach, Anal. Bioanal. Chem. 13 (2017) 3281–3288, doi:10.1007/s00216-017-0296-8.
[22] S. Vahur, U. Knuutinen, I. Leito, ATR-FT-IR spectroscopy in the region of 500–230 cm^{-1} for identification of inorganic red pigments, Spectrochim. Acta - Part A Mol. Biomol. Spectrosc. 73 (2009) 764–771, doi:10.1016/j.saa.2009.03.027.
[23] E.L. Kendix, S. Prati, R. Mazzeo, E. Joseph, G. Sciutto, C. Fagnano, Far infrared spectroscopy in the field of cultural heritage, E-Preservation Sci. 7 (2010) 8–13.
[24] S. Vahur, A. Teearu, I. Leito, ATR-FT-IR spectroscopy in the region of 550–230 cm^{-1} for identification of inorganic pigments, Spectrochim. Acta - Part A Mol. Biomol. Spectrosc. 75 (2010) 1061–1072, doi:10.1016/j.saa.2009.12.056.
[25] P. Giménez, A. Linares, C. Sessa, H. Bagán, J.F. García, Capability of Far-Infrared for the selective identification of red and black pigments in paint layers, Spectrochim. Acta - Part A Mol. Biomol. Spectrosc. 266 (2022) 1–11, doi:10.1016/j.saa.2021.120411.
[26] D. Buti, F. Rosi, B.G. Brunetti, C. Miliani, In-situ identification of copper-based green pigments on paintings and manuscripts by reflection FTIR, Anal. Bioanal. Chem. 405 (2013) 2699–2711, doi:10.1007/s00216-013-6707-6.
[27] P. Griffiths, L. De Haseth, Fourier Transform Infrared Spectrometry, 2nd ed., Wiley, 2007 ed.New Jersey.
[28] C. Invernizzi, L. de Ferri, V. Comite, P. Fermo, M. Malagodi, G. Pojana, Correlation between surface roughness and spectral features in IR-reflection spectroscopy, Microchem. J. 172 (2022) 106874, doi:10.1016/j.microc.2021.106874.
[29] L. Mora, P. Mora, G. Zander, Coloriture e intonaci nel mondo antico - Bollettino d'Arte, Ministero per i Beni e le Attività Culturali. http://www.bollettinodarte.beniculturali.it/opencms/multimedia/BollettinoArteIt/documents/1372164531315_08_-_Laura_Mora.....pdf - (accessed 10 September 2022).
[30] N. Eastaugh, V. Walsh, T. Chaplin, R. Siddall, Pigment Compendium - A Disctionary and Optical Microscopy of Historical Pigments, Elsevier, 2013, doi:10.4324/9780080454573.
[31] F. Volpi, G. Fiocco, T. Rovetta, et al., New insights on the stradivari "coristo" mandolin: a combined non-invasive spectroscopic approach, Appl. Sci. 11 (2021) 1–11, doi:10.3390/app112411626.
[32] M. Vagnini, F. Gabrieli, A. Daveri, D. Sali, Handheld new technology Raman and portable FT-IR spectrometers as complementary tools for the in situ identification of organic materials in modern art, Spectrochim. Acta - Part A Mol. Biomol. Spectrosc. 176 (2017) 174–182, doi:10.1016/j.saa.2017.01.006.
[33] J. Cooper, M. Abdelkader, K. Wise, Sequentially shifted excitation Raman spectroscopy: novel algorithm and instrumentation for fluorescence-free Raman spectroscopy in spectral space, Appl. Spectrosc. 67 (2013) 973–984, doi:10.1366/12-06852.
[34] J. Cooper, S. Marshall, R. Jones, M. Abdelkader, K.L. Wise, Spatially compressed dual-wavelength excitation Raman spectrometer, Appl. Opt. 53 (2014) 3333–3340, doi:10.1364/AO.53.003333.
[35] V. Košařová, D. Hradil, I. Němec, et al., Microanalysis of clay-based pigments in painted artworks by the means of Raman Spectrosocpy, J. Raman Spectrosc. 44 (2013) 1570–1577, doi:10.1002/jrs.4381.

[36] I.M. Cortea, L. Ghervase, R. Rădvan, G. Seriţan, Assessment of easily accessible spectroscopic techniques coupled with multivariate analysis for the qualitative characterization and differentiation of earth pigments of various provenance, Minerals 12 (2022) 755, doi:10.3390/min12060755.
[37] D.L.A. Faria, F.N. Lopes, Heated goethite and natural hematite: can Raman spectroscopy be used to differentiate them? Vib. Spectrosc. 45 (2007) 117–121, doi:10.1016/j.vibspec.2007.07.003.
[38] G. Cavallo, M.P. Riccardi, R. Zorzin, Powder diffraction of yellow and red natural earths from Lessini Mountains in NE Italy, Powder Diffr. 30 (2015) 122–129.
[39] I.M. Cortea, L. Ratoiu, L. Ghervase, O. Ţentea, M. Dinu, Investigation of ancient wall painting fragments discovered in the Roman baths from Alburnus Maior by complementary non-destructive techniques, Appl. Sci. 11 (2021) 1–19, doi:10.3390/app112110049.
[40] M.L. Amadori, S. Barcelli, F. Ferrucci, G. Poldi, Invasive and non-invasive analyses for knowledge and conservation of Roman wall paintings of the Villa of the Papyri in Herculaneum, Microchem. J. 118 (2015) 183–192, doi:10.1016/j.microc.2014.08.016.
[41] H. Helwig, Iron oxide pigments. Natural and synthetic, in: B Berrie, B. Berrie (Eds.), Artists'pigments. A Handbook of Their History and Characteristics, Vol. 4, 2007, pp. 39–109. London.
[42] C. Genestar, C. Pons, Earth pigments in painting: characterisation and differentiation by means of FTIR spectroscopy and SEM-EDS microanalysis, Anal. Bioanal. Chem. 382 (2005) 269–274, doi:10.1007/s00216-005-3085-8.
[43] C.E. Silva, L.P. Silva, H. Edwards, L. De Oliveira, Diffuse reflection FTIR spectral database of dyes and pigments, Anal. Bioanal. Chem. 386 (2006) 2183–2191, doi:10.1007/s00216-006-0865-8.
[44] C. Miliani, F. Rosi, A. Daveri, B.G. Brunetti, Reflection infrared spectroscopy for the non-invasive in situ study of artists' pigments, Appl. Phys. A Mater. Sci. Process. 106 (2012) 295–307, doi:10.1007/s00339-011-6708-2.
[45] P.K. Krivoshein, D.S. Volkov, O.B. Rogova, M.A. Proskurnin, FTIR photoacoustic spectroscopy for identification and assessment of soil components: chernozems and their size fractions, Photoacoustics 18 (2020) 100162, doi:10.1016/j.pacs.2020.100162.
[46] L. Nodari, P. Ricciardi, Non-invasive identification of paint binders in illuminated manuscripts by ER-FTIR spectroscopy: a systematic study of the influence of different pigments on the binders' characteristic spectral features, Herit. Sci. 7 (2019) 1–13, doi:10.1186/s40494-019-0249-y.
[47] C. Ricci, C. Miliani, B.G. Brunetti, A. Sgamellotti, Non-invasive identification of surface materials on marble artifacts with fiber optic mid-FTIR reflectance spectroscopy, Talanta 69 (2006) 1221–1226, doi:10.1016/j.talanta.2005.12.054.
[48] J. Workman Jr, L. Weyer (Eds.), Practical Guide to Interpretative Near-Infrared Spectroscopy CRC Press, Boca Raton, 2007 ByISBN 9781574447842.
[49] V.C. Farmer. The Infrared Spectra of Minerals. (Farmer VC, ed.). London: Mineralogical Society of Great Britain and Ireland. 1974.
[50] P. Cambier, Infrared study of goethites of varying crystallinity and particle size: I. Interpretation of OH and lattice vibration frequencies, Clay Miner. 21 (1986) 191–200, doi:10.1180/claymin.1986.021.2.09.
[51] M. Vagnini, C. Miliani, L. Cartechini, P. Rocchi, B.G. Brunetti, A. Sgamellotti, FT-NIR spectroscopy for non-invasive identification of natural polymers and resins in easel paintings, Anal. Bioanal. Chem. 395 (2009) 2107–2118, doi:10.1007/s00216-009-3145-6.
[52] J.P. Ogalde, C.O. Salas, N. Lara, P. Leyton, C. Paipa, C. Campos-Vallette, B. Arriazza, Multi-instrumental identification of orpiment in archaeological mortuary contexts, J. Chil. Chem. Soc. 59 (2014) 2571–2573, doi:10.4067/S0717-97072014000300010.
[53] *Pictura tacitum poema*Miti e Paesaggi Dipinti Nelle Domus Di Cremona, 2023 Catalogo della mostra a cura di E. Mariani, N. Cecchini, M. VolontèAnte Quem, Cremona. ISBN 9788878491830.
[54] Y. Kim, M.C. Caumon, O. Barres, A. Sall, J. Cauzid, Identification and composition of carbonate minerals of the calcite structure by Raman and infrared spectroscopies using portable devices, Spectrochim. Acta - Part A Mol. Biomol. Spectrosc. 261 (2021) 119980, doi:10.1016/j.saa.2021.119980.
[55] T. Rovetta, C. Invernizzi, G. Fiocco, et al., The case of Antonio Stradivari 1718 ex-San Lorenzo violin: history, restorations and conservation perspectives, J. Archaeol. Sci. Reports 23 (2019) 443–450, doi:10.1016/j.jasrep.2018.11.010.
[56] V. Guglielmi, V. Comite, M. Andreoli, F. Demartin, C.A. Lombardi, P. Fermo, Pigments on Roman wall painting and stucco fragments from the Monte d'Oro Area (Rome): a multi-technique approach, Appl. Sci. 10 (2020) 1–18, doi:10.3390/app10207121.